

Improvements in Resolution of ^1H NMR of Solids

Bruno Simões de Almeida[§] and Lyndon Emsley^{*}

[§]SCS-Metrohm Award for best oral presentation in Analytical Sciences

Abstract: Magic angle spinning (MAS) in ^1H NMR has allowed progress from featureless spectra in static samples to linewidths of a few hundreds of Hertz for powdered solids at the fastest spinning rates available today (100–150 kHz). While this is a remarkable improvement, this level of resolution is still limiting to the widespread use of ^1H NMR for complex systems. This short review will discuss two recent alternative strategies that have significantly improved ^1H resolution, when combined with fast MAS. The first is based on anti-z-COSY, a 2D experiment originally used for J decoupling in liquids, which removes residual broadening due to splittings caused by imperfect coherent averaging of MAS. The second strategy is to obtain pure isotropic proton (PIP) spectra in solids, by parametrically mapping any residual broadening due to imperfect averaging into a second dimension of a multidimensional correlation spectrum.

Keywords: Magic angle spinning anti-z COSY · PIP · Solid-state NMR



Bruno Simões de Almeida is a PhD student in the Laboratory of Magnetic Resonance under the supervision of Prof. Lyndon Emsley at the Ecole Polytechnique Fédérale de Lausanne (EPFL). His research focuses on the development of methods to improve the resolution of ^1H NMR in solids with magic-angle spinning (MAS), and on theoretical studies of the spin behaviour under MAS. He studied Chemistry (BSc) at

the University de Genève and Chemoinformatics (MSc) at the Université de Strasbourg.



Lyndon Emsley is a Professor of Physical Chemistry and the head of the Magnetic Resonance Laboratory at EPFL. His research focus is on the development of new NMR spectroscopy experiments to determine atomic-level structure and dynamics of complex materials and molecular systems.

1. Introduction

NMR of solids is one of the strongest techniques for structure elucidation, and its applications range over a large variety of materials, from batteries and cements to biomolecules and pharmaceuticals.^[1] For many of these cases, ^1H would be the nucleus of choice due to its high natural abundance and chemical shift range. However, obtaining useful structural information from ^1H NMR spectra of solids remains a challenge. The presence of strong ^1H – ^1H dipolar interactions combined with the natural abundance of protons typically result in linewidths of several kHz, obscuring the underlying chemical shifts and making resonance

assignment impossible. The development of methods to improve the resolution of ^1H spectra would substantially reinforce the role of solid-state NMR in the field of structural characterization. The introduction of coherent averaging approaches allowed the selective modulation and elimination of particular spin interaction terms. The prime examples are the spin echo,^[2] which removes the chemical shift, and the heteronuclear decoupling of J couplings in solution state.^[3] In solid-state NMR, the essential coherent averaging method is magic angle spinning (MAS),^[4] which consists of physically spinning the sample around an axis tilted at 54.74° with respect to the main magnetic field. At this angle, all interactions having a second rank spatial dependence (such as dipolar couplings) are averaged out completely, in the limit of infinitely fast spinning, while the isotropic chemical shifts are preserved. With MAS, the resolution in ^1H spectra is typically improved by two orders of magnitude when compared to spectra of static samples. On top of MAS, techniques combining rotation and multi-pulse spectroscopy (CRAMPS) have improved the homonuclear decoupling.^[5] The use of the simultaneous application of MAS and pulse sequences improve the ^1H linewidths using spinning rates up to 65 kHz.^[6] At faster rates, no considerable improvement has been shown so far with CRAMPS approaches. Nevertheless, even at the fastest MAS rates available today (around 100–150 kHz),^[7] proton linewidths are still a few hundred Hz broad, which, in many cases, is still very limiting to resolve ^1H resonances. On the other hand, ^1H linewidths in solution NMR spectra are typically 1 Hz broad. The residual broadening in ^1H NMR of solids comes from different sources. Some of them are independent of MAS, such as B_0 field inhomogeneity, anisotropic bulk magnetic susceptibility^[8] and chemical shift dispersion due to structural disorder of the sample. On the other hand, the imperfect nature of the coherent averaging by MAS, either due to the misset of the magic angle or due to the finite speed of spinning, results in residual shift and splitting

^{*}Correspondence: Prof. L. Emsley, E-mail: lyndon.emsley@epfl.ch

Institut des Sciences et Ingénierie Chimiques, Ecole Polytechnique Fédérale de Lausanne (EPFL), CH-1015 Lausanne, Switzerland

terms^[9] that broaden the spectrum and can only be completely averaged out at infinite MAS rate.

In this review, the aim is to discuss two alternative approaches to any previous strategies based on coherent averaging, which produce narrower ¹H proton spectra. The first requires a 2D experiment that only generates correlations involving a spin state flip of the coupling partners, *i.e.* remote transitions. This approach allows to remove any residual splittings under MAS with a 45° projection of an anti-z-COSY spectrum.^[10] The second approach consists on an error mapping approach where all the residual broadening terms due to imperfect MAS are removed and the isotropic spectra for different organic solids is obtained.^[11] The text here is largely adapted from references [17] and [18].

2. Anti-z COSY

Originally introduced by Oschkinat *et al.*^[12] to probe correlation between remote transitions, the anti-z-COSY pulse sequence (Fig. 1) was then used for homonuclear J decoupling in liquid-state NMR.^[13] Remote transitions occur when passive spins (coupling partners) invert their spin state in t_2 with respect to that in t_1 . The result of this sequence is a phase sensitive z-filtered COSY-like 2D spectrum. The selection of correlations between remote transitions is dependent on the pulse angles β (Fig. 1). As this angle approaches zero, the structure of the diagonal peak is solely composed of remote correlations. These correlations correspond to peaks lying along a line perpendicular to the diagonal.

Fig. 1 compares the 1D ¹H spectrum obtained from a 45° projection across the diagonal peaks from the anti-z-COSY spectrum with the conventional echo-detected MAS spectrum for a sample of powdered thymol. Both spectra were acquired at 100 kHz MAS. The anti-z-COSY spectrum has peaks that are narrower by up to a factor of two. The resolution improvement is due to the removal of the residual splitting terms caused by the anti-z COSY sequence. However, the residual shift terms are retained.

Decreasing β increases the ratio between the wanted anti-diagonal peaks and the other peaks in the multiplet, but at the same time the overall intensity of the correlations also decreases. The flip-angle dependence is showcased in Fig. 1c–f, which show the thymol linewidths for β angles from 90° to 3°. In the spectrum with $\beta = 3^\circ$, for H1, H2, H3, and H4 of thymol, the corresponding linewidths are 208, 194, 245 and 218 Hz. For $\beta = 90^\circ$, they are 359, 336, 350, and 346 Hz. The resolution improvement factor ranges from 1.4 to 1.7. Fig. 2 presents the results for β -AspAla, which shows again the decoupling effect as observed for thymol above.

Another important factor to take into consideration when implementing an anti-z COSY experiment is to keep the z magnetization fixed during the z-filter period. Any effect changing any of the spin states during the mixing scheme, especially spin diffusion, results in a reduction in resolution. Although faster spinning rates slow down homonuclear spin diffusion, the delay should be kept as short as possible. Here a mixing time equal to a single rotor period (10 μ s) is used.

In short, the anti-z COSY sequence is able to improve the homonuclear decoupling in organic solids by exclusively selecting remote correlations. The resolution improvement factor can go up to two, when compared to conventional echo-detected MAS experiments.

3. Pure Isotropic Proton (PIP)

The second approach to increasing ¹H resolution is based on parametrically mapping the residual broadening terms due to imperfect MAS, so they can be separated from the isotropic signal in a multidimensional correlation experiment.^[11] In 2D NMR spectroscopy or imaging, there are normally two time periods. They are usually independently sampled and are represented as

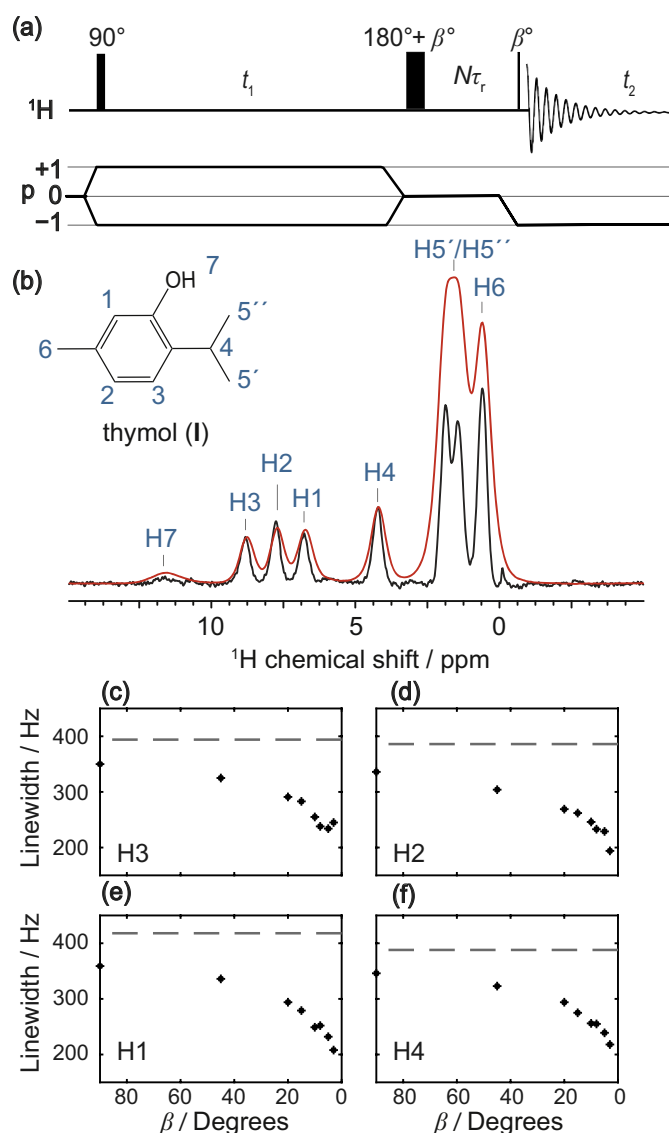


Fig. 1. a) Pulse sequence and the coherence-transfer pathway of anti-z COSY, where β corresponds to small flip angle pulse. b) Echo-detected spectrum (red) and 45° projection of an anti-z COSY spectrum with a flip angle of 5° (black) of thymol acquired with 100 kHz MAS. c–f) Linewidths of protons H1–H4 from anti-z COSY spectra of thymol as a function of β acquired at 100 kHz MAS. The dashed lines represent the protons linewidths measured in the spin-echo spectrum. Figure adapted from ‘Homonuclear Decoupling in ¹H NMR of Solids by Remote Correlation’^[17] by P. Moutzouri *et al.*, used under CC BY 4.0.

orthogonal directions (k_x and k_y) in reciprocal k-space.^[14] Different methods have been developed to sample the k-space.^[14,15] In the PIP experiment, the k-space contains one axis representing the evolution of the isotropic interaction in a coherent averaging experiment, and the other axis represents the error terms evolution, which include all errors generated by the imperfect MAS coherent averaging.^[11] Every FID will then evolve along a straight line in this k-space, at an angle φ to the vertical axis, where φ is dependent on the scaling factor of the error terms.

To fill the k-space, we consider a set of FIDs from a series of MAS spectra obtained at different spinning rates. In these spectra, evolution due to the isotropic part will be constant, but the evolution due the error terms will be scaled, resulting in a change in the angle φ from one FID to another, as shown in Fig. 3. Currently, it is not possible to spin faster than 100–150 kHz, and the k-space cannot be completely sampled (otherwise the experiment here would not be required!). Transforming the 2D

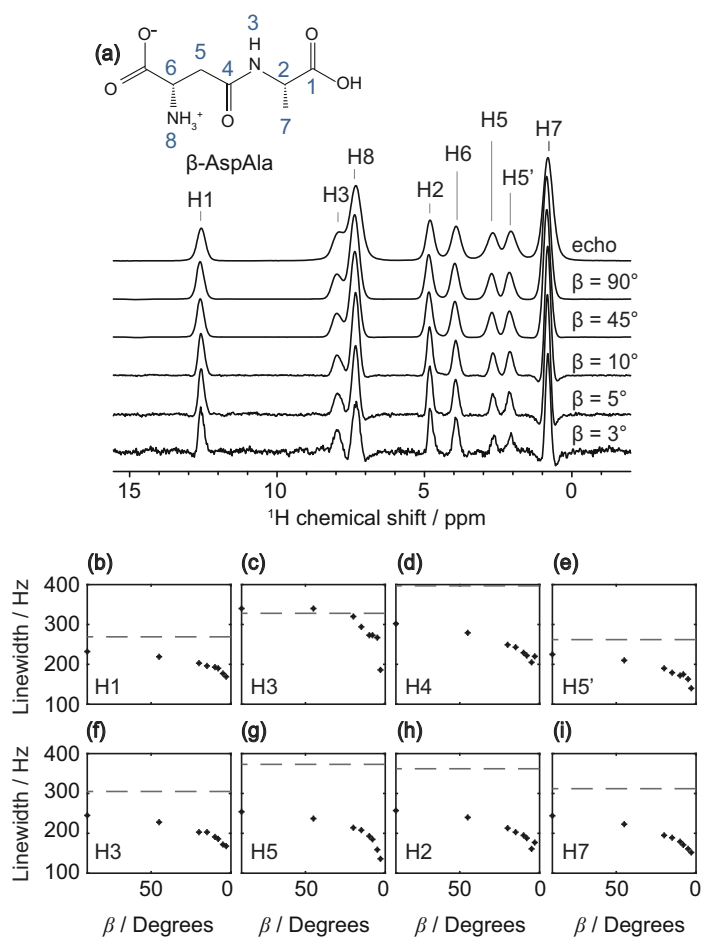


Fig. 2. a) 45° integral projections of β -AspAla from anti-z-COSY spectra acquired at 100 kHz MAS. The top spectrum is the spin-echo at 100 kHz MAS. b)–i) H1–H7 measured linewidths as a function of β . The dashed lines correspond to the proton linewidths measured in the spin-echo spectrum. Figure adapted from 'Homocoupling in ^1H NMR of Solids by Remote Correlation'^[17] by P. Moutzouri *et al.*, used under CC BY 4.0.

variable rate MAS dataset, and taking the projection onto the pure isotropic axis, is thus not straightforward. There are probably many ways to approach this problem. As a proof of concept, the parameter fitting approach summarized in Fig. 4 can be used.

A 2D dataset of MAS spectra acquired at different rates can be fit to the isotropic profile (an amplitude vector), the residual broadening parameters and the residual shift.

Fig. 4 explains the model and the fitting approach with a 2D synthetic data set created by convolution of a random isotropic profile (red) with the broadening function (orange). 128 points are fitted, and the model brings out the isotropic spectrum, reproducing the initial function. By only fitting the broadening due to MAS, the model makes no prior assumption about the underlying nature of the isotropic spectrum. In principle, this one can take form of any shape.

The approach was applied to six different compounds: L-tyrosine hydrochloride, β -AspAla, L-histidine hydrochloride monohydrate, thymol, flutamide, and ampicillin (Fig. 5). For each one of them, a 2D dataset of spectra was obtained at MAS rates going from 20 to 100 kHz. To reduce the computational requirements, the spectrum was divided into subregions, where each region is associated to a unique set of shift and broadening fitting parameters. The improvement in resolution is spectacular for all the pure isotropic spectra obtained. The narrowing is evident for many peaks, but there are also resolved which were broad in the 100 kHz MAS spectrum. For these samples,

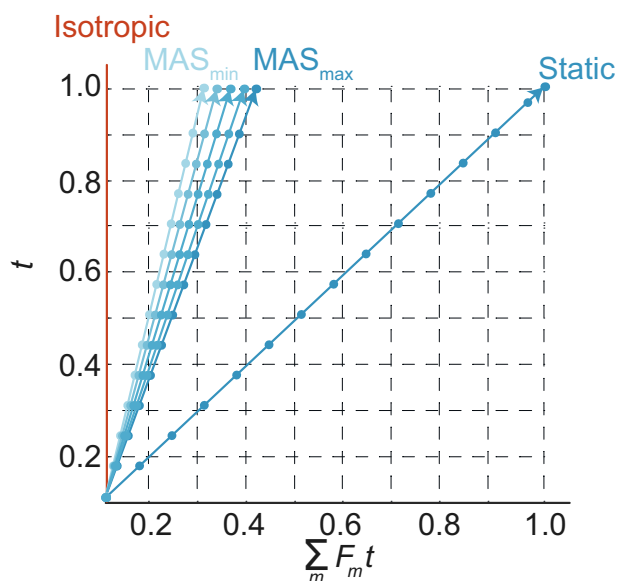


Fig. 3. Graphic description of a series of NMR data acquired at various MAS rates in a k-space where $k_x = \sum_m F_m t$ and $k_y = t$.^[11] Lines represent FIDs obtained at different MAS rates, and dots show sampling points. The line at 45° corresponds to a static sample and the pure isotropic FID would lie along the vertical axes, shown in red. Figure adapted from 'Pure Isotropic Proton Solid State NMR'^[18] by P. Moutzouri *et al.*, used under CC BY 4.0.

the resolution improvement factors are estimated between 1.2 and 20, with an average value of 7. The narrowest lines in the spectra are 48 Hz broad, which corresponds to twice the digital resolution limit.

The resolving power is particularly evident in the 0–3 ppm region of the spectrum of thymol where the signals from the three methyl groups, H5, H5', and H6 are clearly resolved in the isotropic spectrum. Similar effects are also observed in the 4–6 ppm region of L-tyrosine hydrochloride and the 3–8 ppm region of ampicillin.

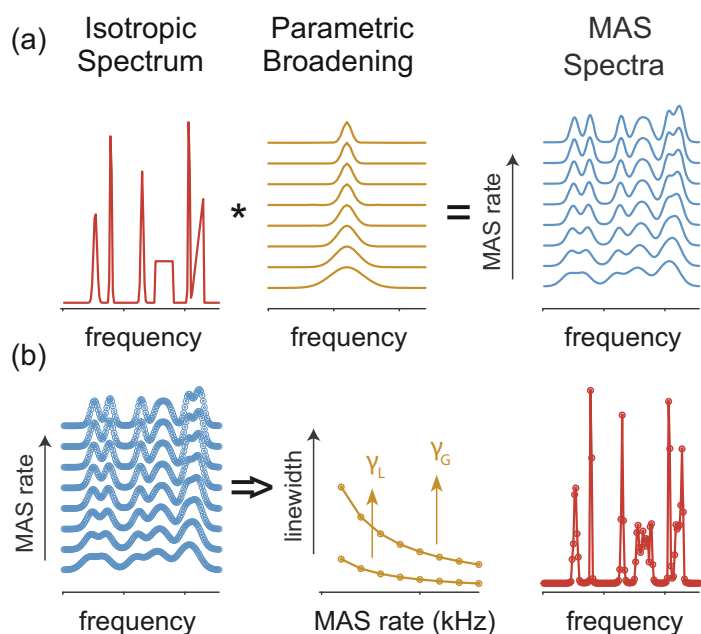


Fig. 4. (a) Schematic representation of the PIP model. Each MAS spectrum (blue) is represented as a convolution of a constant pure isotropic spectrum (red) with a weighting function (orange) that describes the MAS rate dependent broadening. (b) Performance of the model on synthetic VS data, with the isotropic spectrum (red) and the broadening factors γ_G and γ_L . Figure adapted from 'Pure Isotropic Proton Solid State NMR'^[18] by P. Moutzouri *et al.*, used under CC BY 4.0.

All of the resolved peaks in these spectra agree with the expectations from previously acquired ^1H - ^{13}C HETCOR spectra.^[11,16] After inspecting all the isotropic lineshapes, it is important to note that the model is not blindly fitting the data to narrow lines. For example, the protons H6, H8, and H9 of L-histidine hydrochloride monohydrate were fit simultaneously in one single subregion. The isotropic lines for H6 and H8 are narrow, but H9 has a broader distribution. The motional broadening related to the amino proton nature of H9 might explain the broader isotropic peak. This was also observed for the H10 proton in L-tyrosine hydrochloride, which is also in an NH_3^+ group.

Along with the expected peaks, there are a few minor peaks that are classified as artifacts. In L-tyrosine hydrochloride, they are present at 4.1 and 7.9 ppm, in flutamide at 0.95 ppm, and in ampicillin in the 0–1 ppm region and at 5.9 ppm. The origin of these artifacts is possibly explained by the approximations in the model, not being able to completely describe the data. While broad lines are not unanticipated, a different reason for the broader lines mentioned above can also be the model failing to fully describe those peaks, for instance, if the lineshapes are not completely symmetric or if the linewidth has MAS dependence not equal to $1/\omega_{\text{MAS}}$.

4. Conclusions

The search for ^1H resolution in solid-state NMR has seen vast efforts over the last years and future developments can only improve its expansion into the structure elucidation field. This short review described two recent strategies to improve the ^1H resolution at fast MAS (100 kHz). The 2D decoupling scheme anti-z COSY removes any residual splitting caused by imperfect MAS and was applied to two different samples, achieving an average resolution improvement factor of ~ 2 . This technique requires spectra with high resolution in the indirect dimension, which can lead to an experimental time of hours. An improved version of this sequence has already produced similar results for resolution, but only requiring an experimental time of minutes.^[17]

The error mapping PIP approach yields a pure isotropic spectrum from a 2D dataset of variable rate MAS spectra. By transforming the data using a parametric fitting method, applied to six different samples, the linewidths were decreased by a factor up to 20, with 48 Hz being the narrowest linewidth measured.

These proof of concept results indicate the potential of PIP, however the different assumptions and inherent restrictions of the fitting approach might limit the model performance. More recently, transformation of the data using a deep learning strategy^[18] has yielded linewidths on par with the fitting approach, while reducing the number of assumptions, and resulting in reduced artifacts (and being less computationally expensive).

At this stage, much further work is now needed to improve the data collection and transformation strategies, and to understand what are the remaining limiting factors to proton resolution in solids.

Acknowledgements

We acknowledge many stimulating discussions with Pinelopi Moutzouri, Daria Torodii, and Manuel Cordova, who contributed greatly to the work reviewed here. We acknowledge Metrohm for sponsoring the SCS 2022 Presentation Award. Financial support from the Swiss National Science Foundation under Grant No. 200020_212046 is acknowledged.

Received: February 21, 2023

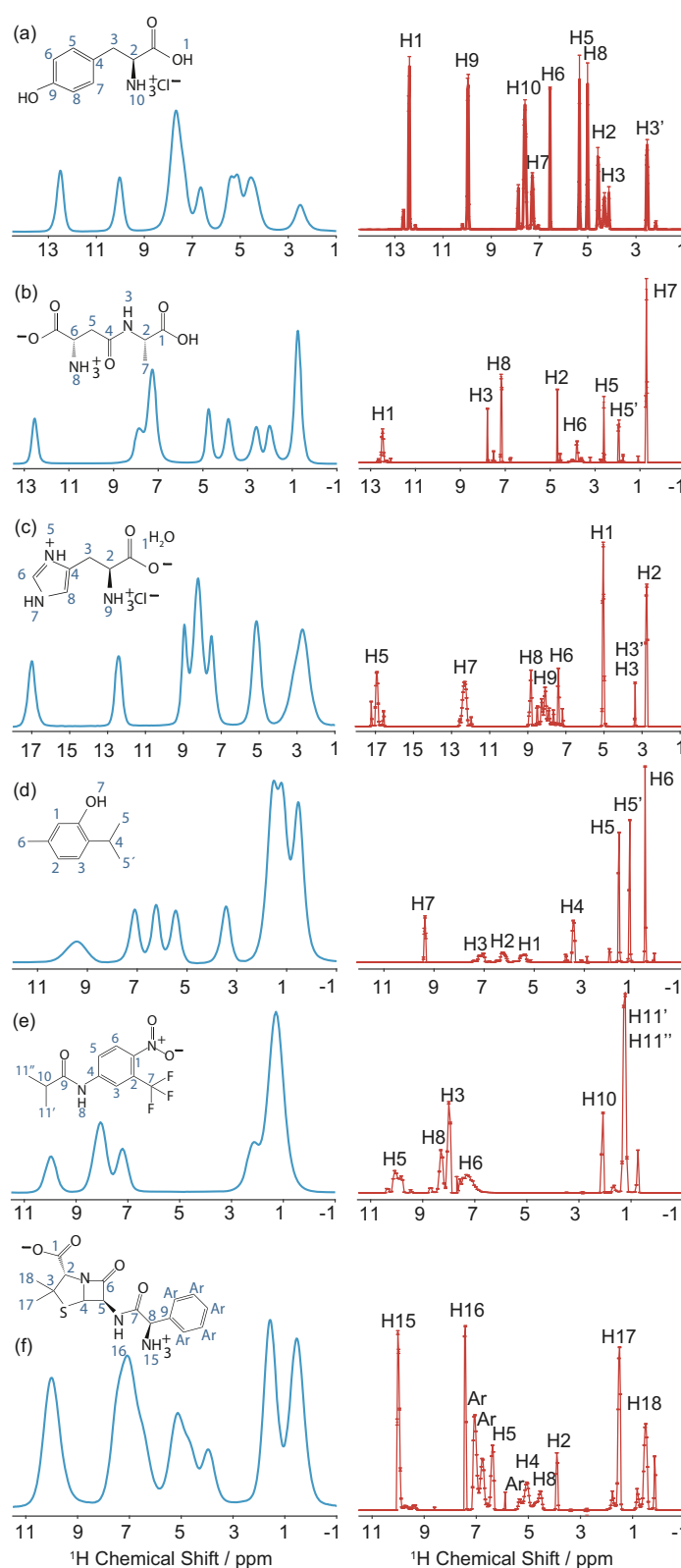


Fig. 5. The 100 kHz MAS spectra (blue) and the average pure isotropic spectra (red) extracted from a 2D dataset of VS data and transformed using the PIP model described in Fig. 3 for powdered samples of (a) L-tyrosine hydrochloride, (b) AspAla, (c) L-histidine hydrochloride monohydrate, (d) thymol, (e) flutamide, and (f) ampicillin. The assignments of the spectra are indicated. Figure adapted from ‘Pure Isotropic Proton Solid State NMR’^[18] by P. Moutzouri *et al.*, used under CC BY 4.0.

[1] B. Reif, S. E. Ashbrook, L. Emsley, M. Hong, *Nat. Rev. Methods Primers* **2021**, *1*, <https://doi.org/10.1038/s43586-020-00002-1>.
 [2] E. L. Hahn, *Phys. Rev.* **1950**, *80*, 580, <https://doi.org/10.1103/PhysRev.80.580>.

[3] a) J. S. Waugh, *J. Magn. Reson.* **1982**, *50*, 30, [https://doi.org/10.1016/0022-2364\(82\)90029-4](https://doi.org/10.1016/0022-2364(82)90029-4); b) A. Shaka, J. Keeler, *Prog. Nucl. Magn. Reson. Spectrosc.* **1987**, *19*, 47, [https://doi.org/10.1016/0079-6565\(87\)80008-0](https://doi.org/10.1016/0079-6565(87)80008-0).

- [4] a) I. J. Lowe, *Phys. Rev. Lett.* **1959**, *2*, 285, <https://doi.org/10.1103/PhysRevLett.2.285>; b) E. R. Andrew, A. Bradbury, R. G. Eades, *Nature* **1958**, *182*, 1659, <https://doi.org/10.1038/1821659a0>.
- [5] a) B. C. Gerstein, R. G. Pembleton, R. C. Wilson, L. M. Ryan, *J. Chem. Phys.* **1976**, *361*, <https://doi.org/10.1063/1.2831927>; b) F. M. Paruzzo, L. Emsley, *J. Magn. Reson.* **2019**, *309*, 106598, <https://doi.org/10.1016/j.jmr.2019.106598>.
- [6] M. E. Halse, L. Emsley, *J. Phys. Chem. A* **2013**, *117*, 5280, <https://doi.org/10.1021/jp4038733>.
- [7] a) T. Kobayashi, K. Mao, P. Paluch, A. Nowak-Król, J. Sniechowska, Y. Nishiyama, D. T. Gryko, M. J. Potrzebowski, M. Pruski, *Angew. Chem.* **2013**, *125*, 14358, <https://doi.org/10.1002/ange.201305475>; b) V. Agarwal, S. Penzel, K. Szekely, R. Cadalbert, E. Testori, A. Oss, J. Past, A. Samoson, M. Ernst, A. Bockmann, B. H. Meier, *Angew. Chem. Int. Ed. Engl.* **2014**, *53*, 12253, <https://doi.org/10.1002/anie.201405730>; c) Y. Nishiyama, M. Malon, Y. Ishii, A. Ramamoorthy, *J. Magn. Reson.* **2014**, *244*, 1, <https://doi.org/10.1016/j.jmr.2014.04.008>; d) Y. L. Lin, Y. S. Cheng, C. I. Ho, Z. H. Guo, S. J. Huang, M. L. Org, A. Oss, A. Samoson, J. C. C. Chan, *Chem. Commun. (Camb)* **2018**, *54*, 10459, <https://doi.org/10.1039/c8cc05882b>.
- [8] a) D. L. VanderHart, W. L. Earl, A. N. Garroway, *J. Magn. Reson.* **1981**, *44*, 361; b) M. Alla, E. Lippmaa, *Chem. Phys. Lett.* **1982**, *87*, 30.
- [9] B. Simoes de Almeida, P. Moutzouri, G. Stevanato, L. Emsley, *J. Chem. Phys.* **2021**, *155*, 084201, <https://doi.org/10.1063/5.0055583>.
- [10] P. Moutzouri, F. M. Paruzzo, B. Simoes de Almeida, G. Stevanato, L. Emsley, *Angew. Chem. Int. Ed. Engl.* **2020**, *59*, 6235, <https://doi.org/10.1002/anie.201916335>.
- [11] P. Moutzouri, B. Simoes de Almeida, D. Torodii, L. Emsley, *J. Am. Chem. Soc.* **2021**, *143*, 9834, <https://doi.org/10.1021/jacs.1c03315>.
- [12] H. Oschkinat, A. Pastore, G. Bodenhausen, *J. Magn. Reson.* **1986**, *69*, [https://doi.org/10.1016/0022-2364\(86\)90176-9](https://doi.org/10.1016/0022-2364(86)90176-9).
- [13] A. J. Pell, R. A. Edden, J. Keeler, *Magn. Reson. Chem.* **2007**, *45*, 296, <https://doi.org/10.1002/mrc.1966>.
- [14] P. T. Callaghan, 'Principles of Nuclear Magnetic Resonance Microscopy', Clarendon Press Oxford, **1991**.
- [15] D. J. States, R. A. Haberkorn, D. J. Ruben, *J. Magn. Reson.* **1982**, *48*, 286, [https://doi.org/10.1016/0022-2364\(82\)90279-7](https://doi.org/10.1016/0022-2364(82)90279-7).
- [16] a) B. Elena, G. de Paëpe, L. Emsley, *Chem. Phys. Lett.* **2004**, *398*, 532, <https://doi.org/10.1016/j.cplett.2004.09.122>; b) A. Lesage, D. Sakellariou, S. Steuernagel, L. Emsley, *J. Am. Chem. Soc.* **1998**, *120*, 13194, <https://doi.org/10.1021/ja983048+>; c) E. D. Salager, G. M. Stein, R. S. Pickard, C. J. Bénédicte, L. Emsley, *J. Am. Chem. Soc.* **2010**, *132*, 2564, <https://doi.org/10.1021/ja909449k>; d) A. Hofstetter, M. Balodis, F. M. Paruzzo, C. M. Widdifield, G. Stevanato, A. C. Pinon, P. J. Bygrave, G. M. Day, L. Emsley, *J. Am. Chem. Soc.* **2019**, *141*, 16624, <https://doi.org/10.1021/jacs.9b03908>; e) P. Bielytskyi, D. Gräising, S. Zahn, A. Alia, J. Matysik, *Appl. Magn. Reson.* **2019**, *50*, 695, <https://doi.org/10.1007/s00723-019-1110-x>; f) M. K. Pandey, R. Zhang, K. Hashi, S. Ohki, G. Nishijima, S. Matsumoto, T. Noguchi, K. Deguchi, A. Goto, T. Shimizu, H. Maeda, M. Takahashi, Y. Yanagisawa, T. Yamazaki, S. Iguchi, R. Tanaka, T. Nemoto, T. Miyamoto, H. Suematsu, K. Saito, T. Miki, A. Ramamoorthy, Y. Nishiyama, *J. Magn. Reson.* **2015**, *261*, 1, <https://doi.org/10.1016/j.jmr.2015.10.003>.
- [17] P. Moutzouri, B. Simoes de Almeida, L. Emsley, *J. Magn. Reson.* **2020**, *321*, 106856, <https://doi.org/10.1016/j.jmr.2020.106856>.
- [18] M. Cordova, P. Moutzouri, B. S. de Almeida, D. Torodii, L. Emsley, *Angew. Chem. Int. Ed. Engl.* **2022**, <https://doi.org/10.1002/anie.202216607>.

License and Terms



This is an Open Access article under the terms of the Creative Commons Attribution License CC BY 4.0. The material may not be used for commercial purposes.

The license is subject to the CHIMIA terms and conditions: (<https://chimia.ch/chimia/about>).

The definitive version of this article is the electronic one that can be found at <https://doi.org/10.2533/chimia.2023.212>